

Electrical switching in Fe/V/MgO/Fe tunnel junctions

N. Najjari, D. Halley, M. Bowen, H. Majjad, Y. Henry, and B. Doudin

IPCMS, UMR 7504, UDS-CNRS, 23 rue du Læss, BP 43, 67034 Strasbourg Cedex 2, France

(Received 2 February 2010; revised manuscript received 29 March 2010; published 25 May 2010)

Bipolar hysteretic resistance switching in epitaxial Fe/V/MgO/Fe magnetic tunnel junctions is observed in highly reproducible $I(V)$ curves and found to be modified by the frequency of the bias voltage sweep. Observation of slow relaxation of the resistance state values is reported. A model is proposed that takes into account the incidence of time-dependent electric-field-induced migration of atomic species on the effective barrier thickness. This model provides a good qualitative agreement with experimental data.

DOI: [10.1103/PhysRevB.81.174425](https://doi.org/10.1103/PhysRevB.81.174425)

PACS number(s): 72.25.Ba, 73.20.Hb, 73.40.Gk, 73.40.Qv

The resistive switching¹ effect has been studied since 1970s in bulk crystals² and for a few years in perovskites³ and binary oxides¹ thick layers. Fewer resistive switching studies have addressed the case of very thin insulating layers used as tunnel barriers, even though they are highly attractive for designing spin electronics devices. Among them, we can mention switching effects in alumina barriers,^{4–6} in perovskites,⁷ in MgO,^{8–11} or NiO.¹² We recently showed switching effect in Fe/Cr/MgO/Fe junctions combined with tunnel magnetoresistive effects.⁹ We attributed this switching to localized defects due to the reversible diffusion of either Cr or O species. Recently, a “memristor” model was put forward by Strukov and co-workers that simulates the effect of electromigration in oxide films in order to explain this switching effect.¹³ In this model, $I(V)$ cycles are represented by distorted Lissajou curves, with a hysteretic opening that is modulated by the frequency of the bias voltage sweep. Systematic studies of the dynamics of the switching process are therefore key to getting better insight into the origin of the resistance switching phenomenon.

In this paper, we investigate ultrathin MgO barrier in epitaxial Fe/V/MgO/Fe magnetic junctions. Relative to their Cr counterparts,⁹ these vanadium-dusted (V-dusted) junctions systematically exhibit reproducible, hysteretic $I(V)$ cycles, defining resistive off and on states. This hysteresis strongly depends upon the frequency of the bias sweep used to generate $I(V)$ curves. We have extended the Strukov model¹³ by introducing a term that takes into account the time-dependent redistribution of chemical species within the junction barrier after modifying the amplitude/sign of the applied electric field. This term reflects our experimental observation of a slow time dependence of the resistance states, modified by the voltage history of the sample.

Heterostructures were deposited by molecular beam epitaxy on (001) MgO substrates in a chamber with a base pressure of 10^{-10} Torr. A 20 nm Fe buffer layer was first deposited at room temperature and annealed at 450 °C for 1 h. The rest of the stack was subsequently grown at 100 °C to prevent interdiffusion between the layers. It consists of an ultrathin layer of V followed by a 3 nm MgO barrier, a 6 nm Fe layer, and a 15 nm layer of Co.¹⁴ The sample was eventually capped with 2 nm of Pt so that the final stacking sequence of our samples is (thicknesses in nm) MgO/Fe(20)/V(d)/MgO(3)/Fe(6)Co(15)/Pt(2), including an epitaxial, bcc (001)-oriented Fe/V/MgO/Fe multilayer junction stack. The crystalline structure of the MgO barrier seems not to be

modified by the underlying thin vanadium layer: reflexion high-energy electron diffraction (RHEED) observations during growth show a layer-by-layer growth of the vanadium and MgO layers, as proved by the specular beam intensity oscillations. Moreover, no roughening of the MgO layer is observed on the RHEED pattern in the presence of the vanadium layer.

Micron-sized junctions were then patterned using standard techniques, including optical lithography, Ar ion etching, SiO_x encapsulation, and lift-off of a Ti/Au bilayer to achieve the top electrical contact.⁹ Transport measurements were performed at room temperature using a conventional four-wire technique. The applied $V(t)$ curves had triangular shapes, imposing therefore a voltage sweep rate of constant magnitude. A fast AD converter (10 Msamples/s, 16 bits), synchronized with an analog sweep generator (up to 250 kV/s), was used to perform the sweep measurements. The reference of positive voltage was taken at the top electrode (with no vanadium). This means that, for a negative bias, negatively charged species such as electrons or oxygen anions may migrate toward the lower junction interface that is dusted with vanadium.

The resistive switching features presented in Fig. 1(a) are representative of 80% of the 50 tested junctions with a vanadium thickness $d=1.2$ nm. Repeated $I(V)$ cycles up to $|V|=1$ V on our Vanadium-dusted junctions reveal a clear hysteretic behavior that leads to a two-level resistance state. The $I(V)$ curves exhibit a continuous hysteretic behavior, with an opening in the cycle that depends on the sweep frequency and on the maximum applied voltage. This hysteretic behavior leads to a resistance decrease for negative bias and to an increase for positive bias. No such hysteresis was observed on reference Fe/MgO/Fe junctions [Fig. 1(b)]. The bipolar switching in the $I(V)$ curves demonstrates a high degree of repeatability (Fig. 2): up to 100 cycles were performed and showed two stable resistance states with a slow relaxation. Their is no electroforming step before observing resistance switching in these junctions: virgin junctions exhibit an hysteretic behavior on $I(V)$ curves even with a low-maximum applied voltage of -0.2 V, for instance.

Above 1 V, the switching regime changes: the resistance switching are abrupt and after a few $I(V)$ cycles, the junction definitively breaks down toward a low resistance. Notice that, before breaking down, in this high-voltage regime—i.e., $|V|>1$ V—the effect of the polarity of the voltage is not

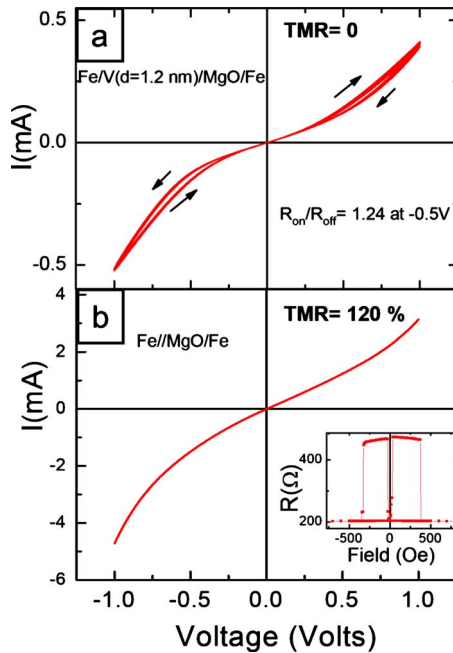


FIG. 1. (Color online) (a) Ten successive $I(V)$ curves on Fe/V/MgO/Fe $20\ \mu\text{m}$ wide circular junction with 1.2 nm vanadium. Each cycle was measured in 100 s. (b) Fe/MgO/Fe $30\ \mu\text{m}$ wide circular junction $I(V)$ curves and (see inset) magneto-resistance measurement at room temperature.

systematic: either the resistance increases with $V > 0$ or it decreases, depending on the measured junction.

We present in Fig. 3 a typical time-dependent resistance trace upon applying a specific series of applied bias voltages. Referring to Fig. 3, we apply a given dc bias V_1 in order to obtain a quasi stationary regime and then we apply a dc bias V_2 to the junction. This leads to a time-dependent resistance that tends toward an upper (lower) limit for a positive (negative) value of $V_2 - V_1$. The presence of this transitory regime clearly shows that the junction history, and more precisely here the junction state prior to the bias change, determines the time-dependent junction response. This relaxation on long time scales was not observed in the case of chromium dusting⁹ but is analogous to what was observed by Krzysteczko *et al.*¹⁵ in MgO barriers.

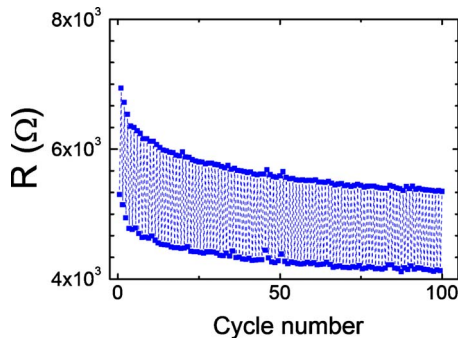


FIG. 2. (Color online) Resistance measured at $+0.6\ \text{V}$ in the “on” and the “off” states as a function of the number of $I(V)$ cycles on a Fe/V/MgO/Fe $10\ \mu\text{m}$ diameter junction with 1.2 nm vanadium. The maximum applied voltage is $\pm 1\ \text{V}$.

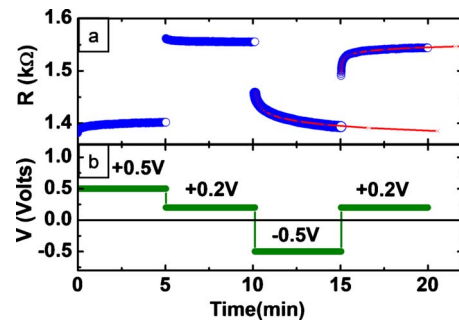


FIG. 3. (Color online) (a) (Dots) Successive resistance measurements versus time at $+0.5$, $+0.2$, and $-0.5\ \text{V}$ on a $25\ \mu\text{m}$ wide circular junction. Regardless of relaxation effects, the resistance value depends on the voltage due to non linear $I(V)$ curves (see Fig. 1). It thus explains the resistance jump when the bias voltage is changed. (Full line) Logarithmic fit of the last two experimental curves. (b) Applied bias voltage.

No magnetoresistance is observed for these junctions with a 1.2 nm vanadium layer. This is due to the filtering effect of the vanadium layer on Δ_1 electrons as in the case of a chromium layer.^{9,14} Indeed, the Δ_1 electrons are 100% spin polarized at Fermi level and have been shown to dominate the tunnel transport through MgO, thus leading to high-tunnel magnetoresistance (TMR) values in usual Fe/MgO/Fe systems. As vanadium do not have Δ_1 states at the Fermi level but about 3.5 eV above the Fermi level,¹⁶ the vanadium layer represents a tunnel barrier for Δ_1 electrons, which are thus filtered away.

Our junctions with no vanadium exhibit TMR values of 150% at 300 K but no resistive switching up to a voltage of 1 V as shown on Fig. 1(b). Between 1 and 1.5 V, they break down irreversibly: whatever the applied voltage, their resistance remains close to a few ohms.

Junctions with an intermediate dusting coverage of vanadium (0.3 nm) exhibit a TMR amplitude of about 60% at 300 K and also switching effects [see Fig. 4(a)]. These effects are observed after applying about 0.5 V to the junctions for a few seconds, which can be regarded as an electroforming step. By varying the maximum applied bias during the $I(V)$ cycle, we can modify the shape of the curve and thus the size of the hysteresis. Hence the value of the conductance measured at a constant and low voltage (10 mV) can be varied in a relatively large range. This enables us to observe the value of the TMR (measured at 10 mV) for different values of the resistance of the junctions [see Fig. 4(b)]. As we already showed in the case of Fe/Cr/MgO/Fe tunnel junctions,⁹ the nearly linear behavior of the TMR as a function of R reveals that there a spin unpolarized memristive current channel flows in parallel with a spin polarized non memristive channel. The addition of the conductance of both channels lead to the linear behavior of TMR as a function of R . One can notice a saturation of the TMR value for large resistances—above $400\ \Omega$ in Fig. 4(b)—perhaps once the nonpolarized conductance channel becomes negligible relative to the conductance of the rest of the junction. The main difference with the Fe/Cr/MgO/Fe case is that, in the case of vanadium dusting, resistive switching appears even for low thickness of the dusting layer. This enables us to observe at the same time a

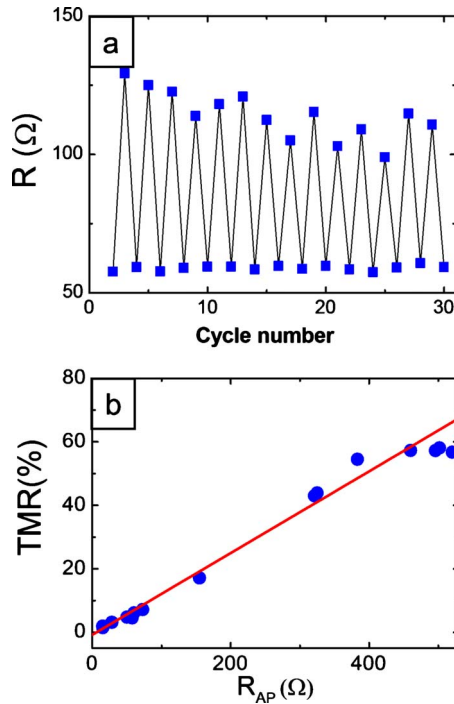


FIG. 4. (Color online) Fe/V/MgO/Fe tunnel junction with a 0.3 nm thick vanadium layer. (a) Resistance measured at +10 mV in the on and the off states as a function of the number of $I(V)$ cycles. The maximum applied voltage during the cycle is ± 0.4 V. (b) TMR measured at 10 mV as a function of the junction resistance at 10 mV in the antiparallel state on a 30 μm diameter junction. A linear fit of the data is shown.

large TMR value (60%) and the switching phenomena. In the case of Cr dusting, the switching effects are weak for $d = 0.3$ nm and the TMR becomes low (in the order of 6%) for thicker dusting layers⁹ exhibiting switching effects.

We should notice that there is a slight evolution of the hysteresis with time on the sample shown on Fig. 4 when modifying the value of the maximum applied voltage. This makes the hysteresis non perfectly reproducible when coming back to a previously measured $I(V)$ curve with a given maximum voltage. This has to be linked with the relaxation of the hysteresis observed on Fig. 2, even without any change of the maximum applied voltage.

Recalling that the hysteretic behavior is not observed in our Fe/MgO/Fe junctions, one can identify the vanadium at the barrier interface as the source of switching. Contrary to the case of Fe/MgO/Fe junctions in which Fe does not seem to be oxidized,¹⁷ V might become oxidized as observed by Cebollada and co-workers in MgO/V/MgO systems.¹⁸ It could then form an additional VO_x insulating barrier¹⁹ next to the MgO one. On the other hand, the oxidation of vanadium might create oxygen vacancies in MgO and thus trapping defects that will influence the tunnel transport through MgO. This has already been observed in the case of Sm (Ref. 20) or Al (Ref. 21) dusting at the interface with insulating oxides: these extra metallic layers can easily oxidize, leading to bipolar switching effects. The required electroforming step in the case of a thin vanadium layer (0.3 nm) suggests that the density of defects leading to the resistive switching de-

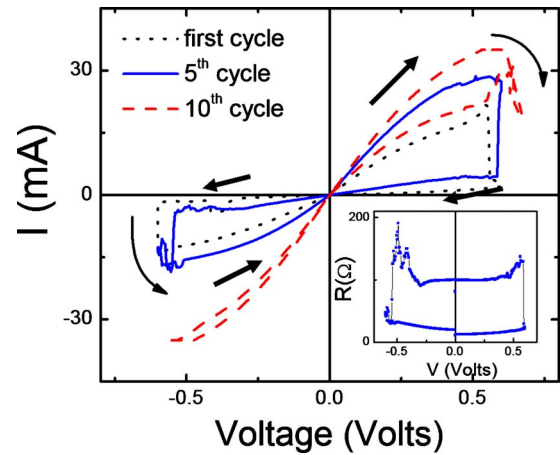


FIG. 5. (Color online) $I(V)$ curves on a 20 μm -wide Fe/MgO/V/Fe circular junction annealed at 450 $^\circ\text{C}$ with 0.06 nm vanadium. The junction evolves irreversibly toward a low resistance state after a few cycles.

pends on the vanadium thickness: with thick vanadium layers, switching defects are present in the barrier even in the virgin state, which is not the case for thinner vanadium layers. The strong effect of a thin vanadium layer on the switching, even stronger than in the case of chromium,⁹ has to be linked with the high oxygen affinity for this metal.²²

Even though we do not observe resistance switching in our non-dusted junctions, some papers reported such effects in Fe/MgO/Fe (Ref. 23) or FeCoB/MgO/FeCoB (Refs. 8, 10, and 11) devices. We have to underline that these reports are only few among the large literature devoted to MgO tunnel barriers, meaning that most of the MgO-based tunnel junctions are stable before breaking down. To explain these reported resistance switching observations in MgO, the question has been raised whether nitrogen contamination in the MgO barrier,²³ or boron diffusion was responsible for instabilities in the $I(V)$ curves. Moreover, oxygen vacancies due to sputtering deposition of the MgO barrier also seem a likely explanation for these effects. Whatever the answer, it seems that the deposition method might explain the appearance of defects in the barrier and the subsequent resistance switching. In our case, with nondusted molecular beam epitaxy (MBE) grown samples, there seem no to be enough defects to induce these resistance switching effects.

In order to enhance the expected oxidation of vanadium at the interface with MgO we have studied annealed systems of Fe/MgO/V/Fe. The annealing was performed before the top Fe layer deposition, in order to avoid Fe-V interdiffusion at high temperature. It was performed at about 450 $^\circ\text{C}$ for 1 h in ultrahigh vacuum, even with low amounts of vanadium— $d = 0.06$ nm—we observe a strong bistability (see Fig. 5) in the $I(V)$ curves. However, the junctions evolve irreversibly toward a low resistance state after a few cycles. This is similar to the high voltage regime—i.e., for $|V| > 1$ V—in our nonannealed samples. Moreover, the effect of the voltage polarity on the resistance behavior varies from one junction to another as in this regime.

These results clearly underscore the strong impact of annealing on enhanced vanadium oxidation and the creation of

defects in MgO. Indeed, in the case of nonannealed samples, no resistance switching is observed for $d=0$, and a reproducible switching is observed for $d=0.3$ nm. Extrapolating these two results to $d=0.06$ nm we expect either no resistance switching or a reproducible resistance switching for this low vanadium thickness in the absence of annealing. The prebreakdown regime in this sample thus proves that the annealing led to the creation of large defects and to the subsequent rapid evolution toward a low-resistance states. We note that 450 °C is close to the optimal annealing temperature in usual MgO-based tunnel junctions.²⁴ Annealing at this temperature cures the intrinsic defects in nondusted MgO barrier. Thus the appearance of strong resistance switching effects after annealing cannot be attributed to the creation of intrinsic defects inside our barriers, but on the contrary, has to be attributed to the oxidation at the MgO/V interface.

For nonannealed samples, we propose to model the hysteretic $I(V)$ curves by taking into account the likely oxidation at MgO interfaces. The observed hysteretic $I(V)$ curves exhibit a continuous change in the junction resistance with no dramatic jumps. This observation is similar to that observed experimentally by Hasan²⁰ or obtained in the model developed by Strukov and co-workers.¹³ In this model, the authors consider the correlated resistivities of two adjacent semiconducting layers, one with a low-doping level and the other one with a high doping level. Electromigration is then supposed to reversibly bring doping atoms from one layer to another, leading to strong changes of the total resistance.

To adapt this model to our V/MgO bilayer system, we suppose that, due to the electric field resulting from the bias voltage V applied across the junction, changes in the junction barrier's microstructure (e.g., the ionic drift of oxygen vacancies and the formation of an effective $\text{VO}_x/\text{MgO}_{1-x}$ barrier) lead to a variation of the effective barrier thickness h , as already made by Ventura *et al.*²⁵ or Krzysteczko *et al.*¹⁵ who supposed constrictions in the tunnel barrier. This does not rule out other hypotheses, such as for instance electron trapping on oxygen vacancies in the barrier or at the interfaces. This indeed would lead to local changes in the potential of the barrier, which also enters in exponential form into the expression of the tunnel conductance. For clarity purposes, we parametrize our model in terms of barrier thickness variations.

Introducing a time dependence of the barrier thickness as: $\frac{dh}{dt} = \alpha V$, with h as the barrier thickness and α as the ionic migration strength. However, this term alone cannot account for the polarity dependence of the transitory regime that we have discussed previously. Indeed, the resistance relaxation should in this case be uniquely defined for a given applied voltage regardless of the junction history, which is not observed in the data of Fig. 3. We actually observe that the sign of the relaxation depends on the sign of the voltage step, i.e., on the difference $V_2 - V_1$. We therefore add a chemical reaction term β that mimics phenomenologically the relaxation of the barrier toward a given thickness h_0 independently of the applied bias. The time dependence of the barrier thickness may now be expressed as

$$\frac{dh}{dt} = \alpha V - \beta(h - h_0). \quad (1)$$

This expression can reproduce the relaxation behavior shown in Fig. 3. Nevertheless, the solution of Eq. (1) in the transitory regime would lead to an exponential decay or growth of the resistance, whereas, as seen from the fits in Fig. 3, the relaxation is logarithmic. It is well known that the sum of exponential contributions with a wide distribution of constants can lead to a logarithmic decay—see, for instance, Ref. 26. In our case, we can suppose large fluctuations of α or β from one defect to another: indeed, the existence of localized defects does not imply that all the defects have the same characteristics—see, for instance, Ref. 27. Suppose for instance electron traps inside the barrier which could be filled or unfilled, so modifying the local conductance: the energy barrier height for trapping an electron could strongly vary from one defect to another, depending on the position of the trap inside the MgO barrier, relative to the V/MgO interface. It would be the same in the case of electromigration: the energy required to move for instance an oxygen vacancy could be modified from one site to another, again as a function of its position inside the MgO barrier. It thus would make sense to suppose a large distribution of parameters α or β , leading to a logarithmic instead of exponential relaxation of the resistance with time. This effect of a large distribution will be detailed in another paper.²⁸

To model our experimental bias sweep, we consider a sinusoidal bias voltage $u = V_0 \cos(\omega \cdot t)$. This leads in the stationary regime to $h = h_0 + \frac{\alpha V_0}{\omega^2 + \beta^2} [\omega \sin(\omega t) + \beta \cos(\omega t)]$. As we showed in the Fe/Cr/MgO/Fe system,⁹ or as shown by Freitas⁴ for alumina barriers, most of the surface area of the barrier should remain unchanged under bias voltage, with atomic migration occurring along local hot-spots in the barrier. We model this as two parallel channels of conductance. Considering the exponential dependence with coefficient γ of the tunneling conductance vs barrier thickness h , the total conductance can be written as $G = G_0 + G_1 e^{[-\alpha \gamma V_0 / (\omega^2 + \beta^2)] [\omega \sin(\omega t) + \beta \cos(\omega t)]} = G_0 + G_1 e^{[-y / (1 + x^2)] [x \sin(\omega t) + \cos(\omega t)]}$ with $x = \omega / \beta$ and $y = \alpha \gamma V_0 / \beta$. G_0 corresponds to the unmodified barrier conductance, while G_1 describes the amplitude of the conductance changes in the defect-mediated channel. For simplicity G_0 and G_1 are taken as constant relative to the bias voltage, which means that we neglect the nonlinearity inherent to the tunnel transport. Taking into account this nonlinearity would simply distort the obtained curves, but would not change the main features of our model. We emphasize here that the additional $\beta \cos(\omega t)$ term leads to asymmetries in the opening ΔI of the $I(V)$ curves, in qualitative agreement with our observations (see Fig. 6).

Assuming a tunnel conductance that varies as $e^{-h\sqrt{2m(E-V)}/\hbar}$, we can evaluate the equivalent thickness change Δh at hot spots within the hypothesis of ionic drift. Here, m is the mass of the electron and E the barrier height. The ratio of the conductance onto defects $G_{\text{defect}} = G - G_0$ in the On and Off states is indeed equal to $e^{-\Delta h\sqrt{2m(E-V)}/\hbar}$ for a given voltage V . From Fig. 6, if we take

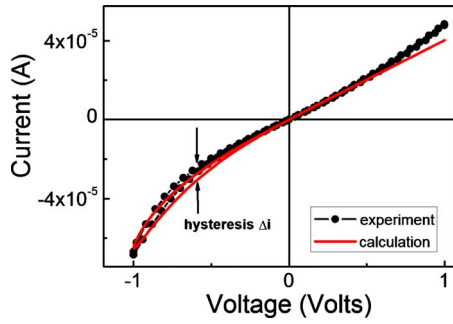


FIG. 6. (Color online) (Dots) Measured asymmetrical $I(V)$ curve on a Fe/V/MgO/Fe with 1.2 nm vanadium. (Line) $I(V)$ curve obtained from the model with $x=0.15$, $y=2.2$, $G_0=3.7 \times 10^{-5}$ S, and $G_1=3.3 \times 10^{-6}$ S.

$G_{\text{defect}}^{\text{On}}/G_{\text{defect}}^{\text{Off}}=1.17$ at -0.7 V, we get $\Delta h=0.03$ nm, with $E-V \sim 1$ eV. Supposing a lower barrier height—for instance a barrier of vanadium oxide—with $E-V \sim 0.1$ eV, we get $\Delta h=0.1$ nm. These values would make sense within the frame of ionic drift since Δh is on the order of the interatomic distance. We have to notice that the 0.03 nm value is in the same order of magnitude as what was found by Krzyteczko *et al.*¹⁵ who estimated the thickness changes in the MgO barrier at 0.01 nm. Moreover, this calculation supposes that all defects behave in the same way, whereas we expect a significant distribution of Δh values: it means that locally, on some hot spots, Δh might be much higher than 0.03 nm. Therefore, due to the exponential dependence of the conductance on the barrier thickness, it would lead to strong local variation of the conductance.

A similar calculation under the hypotheses of barrier height changes and a constant thickness would lead to a 20 meV change for E between the on and off states, which is also realistic. This is for instance of the same order of magnitude as the charging energy for one electron in the case of Coulomb blockade in a tunnel barrier.²⁹

Another consequence can be drawn from our model: In contrast to the model developed by Strukov *et al.*,¹³ the $I(V)$ hysteresis depends in a nonmonotonous manner on ω as shown in Fig. 7(a). Indeed, as long as $\omega \ll \beta$, the hysteretic opening ΔI in the $I(V)$ trace increases with increasing ω , and then decreases when $\omega \sim \beta$, with a maximum value that depends on the bias voltage. This maximum is observed experimentally [see Fig. 7(b)] at positive bias. This clearly indicates that the memristor model as developed by Strukov *et al.* would not be sufficient to describe our frequency-dependent observations. It supports the phenomenological model given by Eq. (1) with the addition of a new term.

The absence of a maximum of the hysteresis under a negative applied bias has nevertheless to be stressed. Our model predicts a maximum at a lower frequency for the

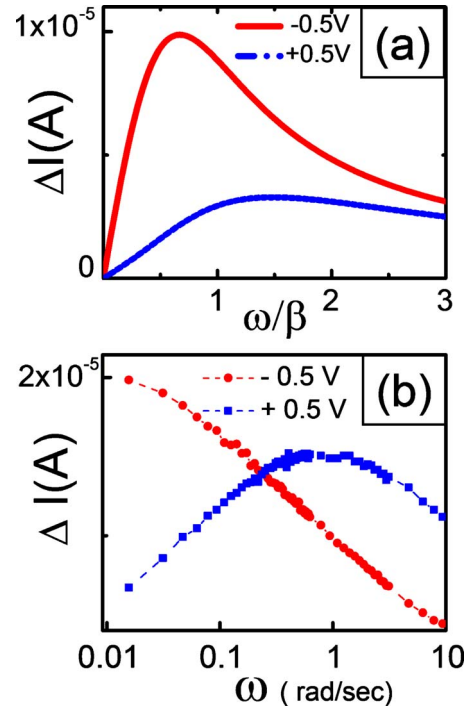


FIG. 7. (Color online) (a) Calculated hysteresis at ± 0.5 V as a function of the normalized sweep frequency ω/β . These values are obtained from the above model with the same set of parameters as in Fig. 6. (b) Experimental hysteresis measured at ± 0.5 V as a function of the voltage sweep frequency ω .

negative polarity [see Fig. 7(a)], but this one should nevertheless be observed. Its absence in experimental observations could for instance be attributed to the distribution of α and β constants, modifying the shape of the curve for this negative polarity.

To conclude, frequency-dependent studies of electrical switching effects in tunnel junctions with MgO barriers and V insertion layers have been modeled with a phenomenological set of equations that captures most of the physical observations by assuming a local change of the barrier thickness or height due to the applied bias voltage. Moreover, this model can describe the experimentally observed asymmetry in the hysteresis of the $I(V)$ curves and the frequency dependence of the hysteretic opening. Relaxation studies reveal that slow processes can be of significant importance, providing insights into the microscopic models for the switching process.

We thank J. Arabski for technical support of the MBE system. N.J. gratefully acknowledges financial support from the Alsace Region.

- ¹R. Waser and M. Aono, *Nature Mater.* **6**, 833 (2007).
- ²T. W. Hickmott, *J. Vac. Sci. Technol.* **6**, 828 (1969).
- ³Y. Watanabe, J. G. Bednorz, A. Bietsch, Ch. Gerber, D. Widmer, A. Beck, and S. J. Wind, *Appl. Phys. Lett.* **78**, 3738 (2001).
- ⁴A. Deac, O. Redon, R. C. Sousa, B. Dieny, J. P. Nozieres, Z. Zhang, Y. Liu, and P. P. Freitas, *J. Appl. Phys.* **95**, 6792 (2004).
- ⁵J. Das, R. Degraeve, H. Boeve, P. Duchamps, L. Lagae, G. Groeseneken, G. Borghs, and J. De Boeck, *J. Appl. Phys.* **89**, 7350 (2001).
- ⁶J. Ventura, A. M. Pereira, J. P. Araujo, J. B. Sousa, Z. Zhang, Y. Liu, and P. P. Freitas, *J. Phys. D* **40**, 5819 (2007).
- ⁷M. Bowen, J.-L. Maurice, A. Barthélémy, P. Prod'homme, E. Jacquet, J.-P. Contour, D. Imhoff, and C. Colliex, *Appl. Phys. Lett.* **89**, 103517 (2006).
- ⁸C. Yoshida, M. Kurasawa, Y. Min Lee, M. Aoki, and Y. Sugiyama, *Appl. Phys. Lett.* **92**, 113508 (2008).
- ⁹D. Halley, H. Majjad, M. Bowen, N. Najjari, Y. Henry, C. Ulhaq-Bouillet, W. Weber, G. Bertoni, J. Verbeeck, and G. Van Tendeloo, *Appl. Phys. Lett.* **92**, 212115 (2008).
- ¹⁰P. Krzysteczko, G. Reiss, and A. Thomas, *Appl. Phys. Lett.* **95**, 112508 (2009).
- ¹¹J. M. Teixeira, J. Ventura, R. Fermento, J. P. Araujo, J. B. Sousa, P. Wisniowski, and P. P. Freitas, *J. Phys. D* **42**, 105407 (2009).
- ¹²A. Sokolov, R. Sabirianov, I. Sabirianov, and B. Doudin, *J. Phys.: Condens. Matter* **21**, 485303 (2009).
- ¹³D. B. Strukov, G. S. Snider, D. R. Stewart, and R. S. Williams, *Nature (London)* **453**, 80 (2008).
- ¹⁴F. Greullet, C. Tiusan, F. Montaigne, M. Hehn, D. Halley, O. Bengone, M. Bowen, and W. Weber, *Phys. Rev. Lett.* **99**, 187202 (2007).
- ¹⁵P. Krzysteczko, X. Kou, K. Rott, A. Thomas, and G. Reiss, *J. Magn. Magn. Mater.* **321**, 144 (2009).
- ¹⁶J. F. Alward, C. Y. Fong, and C. G. Sridhar, *Phys. Rev. B* **18**, 5438 (1978).
- ¹⁷H. L. Meyerheim, R. Popescu, N. Jedrecy, M. Vedpathak, M. Sauvage-Simkin, R. Pinchaux, B. Heinrich, and J. Kirschner, *Phys. Rev. B* **65**, 144433 (2002).
- ¹⁸E. Román, Y. Huttel, M. F. López, R. Gago, A. Climent-Font, A. Muñoz-Martín, and A. Cebollada, *Surf. Sci.* **600**, 497 (2006).
- ¹⁹M. J. Lee, Y. Park, D. S. Suh, E.-H. Lee, S. Seo, D.-C. Kim, R. Jung, B.-S. Kang, S.-E. Ahn, C. B. Lee, D. H. Seo, Y.-K. Cha, I.-K. Yoo, J.-S. Kim, and B. H. Park, *Adv. Mater. (Weinheim, Ger.)* **19**, 3919 (2007).
- ²⁰M. Hasan, R. Dong, H. J. Choi, D. S. Lee, D.-J. Seong, M. B. Pyun, and H. Hwang, *Appl. Phys. Lett.* **92**, 202102 (2008).
- ²¹S. L. Li, D. S. Shang, J. Li, J. L. Gang, and D. N. Zheng, *J. Appl. Phys.* **105**, 033710 (2009).
- ²²R. C. Weast, *Handbook of Chemistry and Physics*, 52nd ed. (Chemical Rubber Company, Boca Raton, FL, 1971).
- ²³S. S. P. Parkin (private communication).
- ²⁴S. Ikeda, J. Hayakawa, Y. Ashizawa, Y. M. Lee, K. Miura, H. Hasegawa, M. Tsunoda, F. Matsukura, and H. Ohno, *Appl. Phys. Lett.* **93**, 082508 (2008).
- ²⁵J. Ventura, J. B. Sousa, Y. Liu, Z. Zhang, and P. P. Freitas, *Phys. Rev. B* **72**, 094432 (2005).
- ²⁶O. B. Tsiok, V. A. Sidorov, V. V. Bredikhin, L. G. Khvostantsev, V. N. Troitskiy, and L. I. Trusov, *Phys. Rev. B* **51**, 12127 (1995).
- ²⁷B. Oliver, G. Tuttle, Q. He, X. Tang, and J. Nowak, *J. Appl. Phys.* **95**, 1315 (2004).
- ²⁸E. Bertin, D. Halley, N. Najjari, and Y. Henry (unpublished).
- ²⁹*Spin Dependent Transport in Magnetic Nanostructures*, edited by S. Maekawa and T. Shinjo (CRC Press, Boca Raton, FL, 2002), Vol. 3, Chap. 4, p. 163.